



DEPARTMENT OF MECHANICAL ENGINEERING

SPECIALIZATION PROJECT

A report on the hybrid metal & extrusion bonding and other cold state welding methods with focus on aluminum to copper bonding

Author:

Peder Sørli Rustad

Abstract

There is an increasing interest in dissimilar metal aluminum (Al) to copper (Cu) welding for various electrical applications. The hybrid metal & extrusion bonding (HYB) method is proposed to be one technique capable of bonding Al to Cu. This report describes and reports on the state of HYB both with regard to Al - Cu bonding as well as other metals. Other weld techniques are described and judged on its capability regarding welding Al - Cu. These include diffusion-, ultrasonic-, friction stir- and cold roll welding. Al - Cu bonding is complicated and combinations of these techniques are being worked on, however, this report does not go into detail on those methods due to the lack of data. An Al - Cu HYB welded joint was hardness tested as well as analyzed in a digital microscope, determining the heat affected zone (HAZ) characteristics and viewing flow patterns with the possibility to detect large defects. A strain hardening was observed on the Cu and a strain softening on the Al base materials (BMs). A total HAZ of 18 mm is observed whereas 6 mm of those occurred in the Cu BM which show an increase in hardness. A preliminary conductivity test was conducted showing promising results for the joint. A preliminary conductivity test was reported with good results, however, cavity defects was discovered in the extrusion zone (EZ) when observing with the electrical microscope.

December, 2020

Contents

1	Introduction	1
1.1	Solid state welding	1
1.2	Al - Cu Intermetallic compounds	2
2	Hybrid metal extrusion and bonding	4
2.1	HYB accomplishments	6
3	Other weld methods	7
3.1	Diffusion welding	7
3.2	Ultrasonic welding	8
3.3	Friction stir welding	9
3.3.1	Flow Patterns in FSW	10
3.4	Cold roll welding	11
4	Experiments	13
4.1	Vickers hardness	13
4.2	Digital microscope and hardness testing	13
4.2.1	specification	13
4.2.2	Procedure	14
4.2.3	Results	15
4.3	Conductivity	18
5	Conclusion	19
5.1	Further work	19
	References	20

1 Introduction

The goal of this report is to find out how well the HYB welding process bond Al to Cu and how it compares to other forms of welding techniques. The price for Al is approximately a quarter that of Cu[1]. Therefore, Al will because of its availability, price advantage and high conductivity, be a very attractive alternative to Cu. Al - Cu electrical joints were originally bolted connections. Bolted connections has a problem with longevity in regard to electrical applications, achieving only a lifetime of around 1 year. Therefore efforts towards bonded joints have been made[2]. Fusion welding is not considered a viable process for these materials due to solidification problems creating brittle intermetallics. Solid state welding techniques are able to mitigate this due to the low operating temperature, and quickly became the standard when bonding Al - Cu[3]. There is interests from both industry and automotive applications when it comes to dissimilar metal welding. Al - Cu joints are used in a variety of applications, for instance bus bars, electrical conductors, refrigeration tubes, tube sheets, capacitor foil windings, transformer's foil conductor and condensers[3].

Property	Copper	Aluminum
Conductivity ($m/\Omega mm^2$)	58	35.5
Density (g/mm^3)	8.93	2.70

Table 1: Conductivity and density properties for Al and Cu[1]

Al - Cu joints are a challenging weld which can be under strenuous and harsh environments, and therefore needs to be durable. A metallurgical bond between these two metals create brittle and electrical resistant intermetallic compounds (IMCs). Expansion coefficient differences between dissimilar metals are one problem which leads to stresses in the bond zone after heating. A relatively low working temperature is preferable when working dissimilar metals. This effect is described in various metal combinations including Al - Cu joints[1, 4].

1.1 Solid state welding

Solid state welding is a method where materials achieves coalescence together and the temperature never reaches the melting point. This is done by either a combination of temperature and pressure or pressure alone. Traditional solid state welding methods does not use any filler material (FM), but may use an interlayer. This includes the methods covered in this report which are diffusion-, friction-, and ultrasonic welding.

Metallurgical bond is created with minimal or no melting of the materials, and can be bonded by either similar or dissimilar materials. The materials are brought together closely so that the atomic forces can attract each other. The surface is an obstacle when it comes to bonding in solid state welding. There can be films of oxidation, oil, gas and so fourth. Fusion welding will solve this by burning or dissolving the film through high temperatures. In solid state welding the temperature is too low for this to happened and the films has to be removed through other means. A surface preparation is often the solution, but some friction based techniques will remove the films during welding, including friction stir welding and HYB[5].

1.2 Al - Cu Intermetallic compounds

Al - Cu welding is problematic due to the metals being incompatible from the welding point of view. IMCs are created because of the high affinity at temperatures above 120 °C. This is also called interdiffusion. IMCs contribute to more brittle mechanical behavior, lower strength as well as greater electrical resistance[6, 7]. It is necessary for the joint to have a wide enough IMC interface for the bond to occur, but not excessive amounts. Braunović and Alexandrov states that mechanical properties radically declines once IMC thickness passes $2\mu m$ [6]. This is substantiated and illustrated in Figure 13, page 12. The phase diagram between Al and Cu has been widely studied and iterations has been done since Murray made a major assessment of the system in 1985[8].

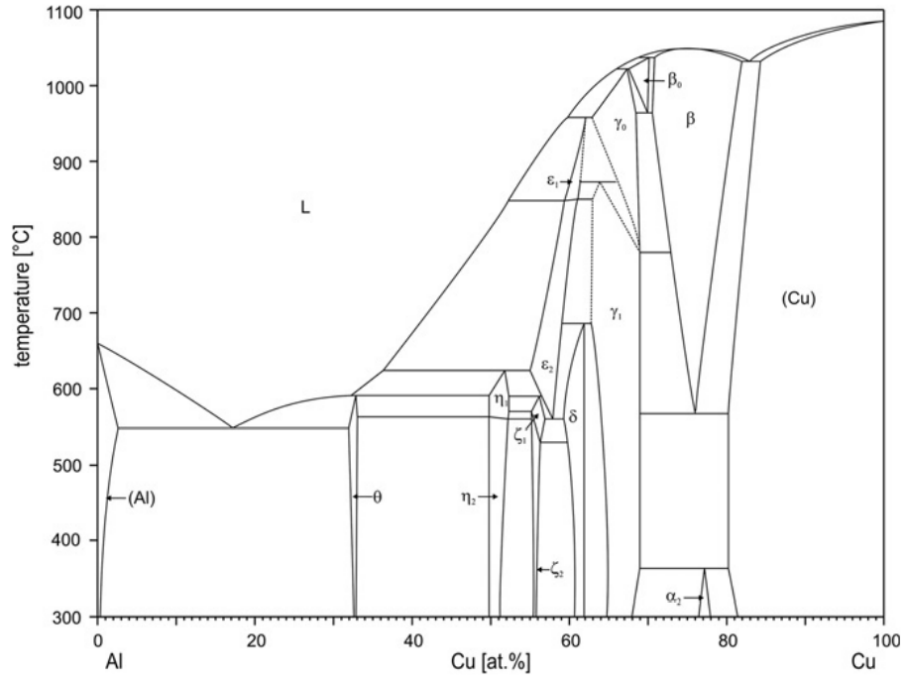


Figure 1: Al-Cu phase diagram[9]

The temperature achieved when HYB welding is around 400°C. Therefore, the IMC structures that can occur during the HYB process are $Al_2Cu(\theta)$, $AlCu(\eta)$, $Al_3Cu_{4-\delta}(\zeta_2)$, Al_4Cu_9 (rhombic)(δ) and $Al_4Cu_9(\gamma_1)$. The different structures are categorized with regard to their symmetry, geometry and composition range in table 2.

Structure	%Cu	PS	SG	Lattice parameters	Reference
Al ₂ Cu	31.9-33.0	<i>tl</i> 12	<i>I</i> 4/ <i>mcm</i>	$a = b = 5.949 \text{ \AA}$ $c = 4.821 \text{ \AA}$ $\alpha = \beta = \gamma = 90^\circ$	[10]
AlCu	49.8-52.3	<i>mC</i> 20	<i>C</i> 2/ <i>m</i>	$a = 11.973 \text{ \AA}$ $b = 4.061 \text{ \AA}$ $c = 6.807 \text{ \AA}$ $\alpha = \gamma = 90^\circ$ $\beta = 124.882^\circ$	[10]
Al ₃ Cu _{4-δ}	55.2-56.3	<i>ol</i> 24 – 3.5	<i>I</i> <i>mm</i> 2	$a = 4.0972 \text{ \AA}$ $b = 7.0313 \text{ \AA}$ $c = 9.9793 \text{ \AA}$ $\alpha = \beta = \gamma = 90^\circ$	[9]
Al ₄ Cu ₉ (r)	59.3-61.9	<i>hR</i> 52	<i>R</i> 3 <i>m</i>	$a = b = c = 8.7066 \text{ \AA}$ $\alpha = 89.74^\circ$ $\beta = \gamma = 90^\circ$	[11]
Al ₄ Cu ₉	52.5-59	<i>cP</i> 52	<i>P</i> – 43 <i>m</i>	$a = b = c = 8.7068 \text{ \AA}$ $\alpha = \beta = \gamma = 90^\circ$	[12]

Table 2: The achievable phases using the HYB method with composition properties, pearson symbol (PS), space group (SP) and lattice parameters

Different weld studies can confirm that the different structures found in the IMC region at various temperatures, conforms with the Al - Cu phase diagram. F. A. Calvo et al. studied the the characteristics of the IMC formation in diffusion welding Al - Cu. The IMCs found in the weld interface were Al₂Cu, AlCu and Al₄Cu₉[13]. These claims are substantiated by the theory on IMC growth between Cu and Al. Interdiffusion can take place after welding as well, if temperatures are elevated. Higher temperatures accelerates the the rate of interdiffusion (*D*). The relationship between the thickness of the IMC structures (*d*) and the time (*t*) is logarithmic shown by equation 1 where *t* is time[6]:

$$d^2 = D \cdot t \quad (1)$$

The nature of the IMCs creates increased resistivity in the joint. The theoretical equation for bimetallic electrical resistivity does not account for the IMCs inherent resistivity. Al - Cu theoretical resistivity is shown in equation 2[4].

$$\frac{1}{\rho_{Ct}} = \frac{\nu_{Al}}{\rho_{Al}} + \frac{\nu_{Cu}}{\rho_{Cu}} \quad (2)$$

ρ_{Al} = Resistivity of Al = $0.0282 \Omega mm^2/m$
 ρ_{Cu} = Resistivity of Cu = $0.0172 \Omega mm^2/m$
 ν_{Al} = Volume fraction of Al = 0.82[4]
 ν_{Cu} = Volume fraction of Cu = 0.12[4]
 ρ_{Ct} = Resistivity of the bimetal

The inverse of the resistivity is the conductivity ($m/\Omega mm^2$), and from this equation we can deduce the theoretical best conductivity. Using a volume fraction of 0.82 for Al and 0.18 for Cu we find the theoretical best conductivity of $39.55 m/\Omega mm^2$ [4]. According to equation 2, the conductivity can not be greater than the Al conductivity, but we know this to be false. In practice the bond has an inherent resistivity which is not accounted for in the formula. Also, all weld defects are affecting the conductivity and it is difficult to differentiate exactly what amount of resistivity is caused by the inherent resistivity of the IMC phases. While cold roll welding Al - Cu, Abbasi et al. highest reached conductivity was $37.61 m/\Omega mm^2$ at IMC thickness close to zero. This closely resembled the theoretical best conductivity[4]. When taking the geometry of the joint into account we can find the resistance. The length of Cu, length of Al and contact surface area are the added variables. The general formula for resistance is shown in equation 3.

$$R = \rho \cdot \frac{l}{A} \quad (3)$$

R = resistance (Ω)

l = length

A = cross section area

One way of solving the resistance for IMCs is to measure how thick (d) each layer of IMC phases are and what resistivity each phase has. In the case of HYB, θ , η , ζ_2 and δ are the phases possible in the interface. Figure 2 illustrates a possible layering of the IMC phases. Assuming each layer has the same interface surface area like Figure 2, equation 4 solves resistance for HYB IMC phases.

$$R_f = \frac{\rho_\theta \cdot d_\theta + \rho_\eta \cdot d_\eta + \rho_\zeta \cdot d_\zeta + \rho_\delta \cdot d_\delta}{A} \quad (4)$$

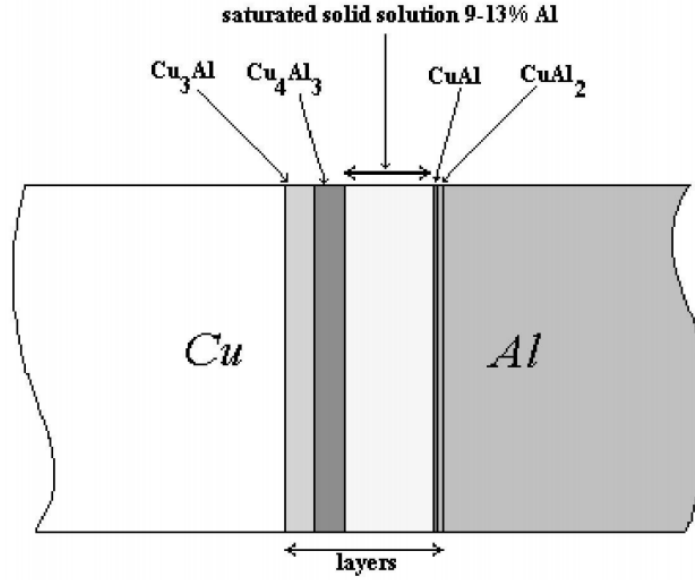


Figure 2: Schematic illustration of possible IMC layers[4]

If the IMC structures aren't separated in layers, the resistivity formula can be utilized to give a general resistivity of the whole IMC layer. The percentage amount of each structure is then needed and used as volume fraction. After this, the length and cross section area of the IMC layer will determine the resistance using equation 3. Equation 5 calculates the IMC layer resistivity for HYB.

$$\frac{1}{\rho_{IMC}} = \frac{\nu_\theta}{\rho_\theta} + \frac{\nu_\eta}{\rho_\eta} + \frac{\nu_\zeta}{\rho_\zeta} + \frac{\nu_\delta}{\rho_\delta} \quad (5)$$

2 Hybrid metal extrusion and bonding

HYB welding is a solid-state joining process where two metal plates or sheets (base materials) are held in place. Butt jointing is the usual procedure, but it has the capability to create both tee joints and corner joints. A gap is left between the two metals which is filled out by a FM. The filled out zone is called the extrusion zone (EZ). A rotating tool extrudes the FM in form of a wire and is pressed down onto and between the metals. The tool inhibits grooves acting as dies where the wire is fed through. As the pin/extrusion head rotates, the wire is fed through due to the friction applied by the grooves. The grooves on the extrusion head are open, which means the wire is exposed to the BMs once it get past the shoulder. The Helicoid-shaped dies on the extrusion head prevents pressure from dropping during welding, an

important mechanism which allows continuous FM extrusion. Velocity of the filler wire (v_w) is given with relation to the spindle radius (r_s), wire slipping in the die (β) and spindle rotation speed (N_s). The relation is shown in equation 6[14].

$$v_w = \beta \cdot N_s \cdot \frac{2\pi r_s}{60} \quad (6)$$

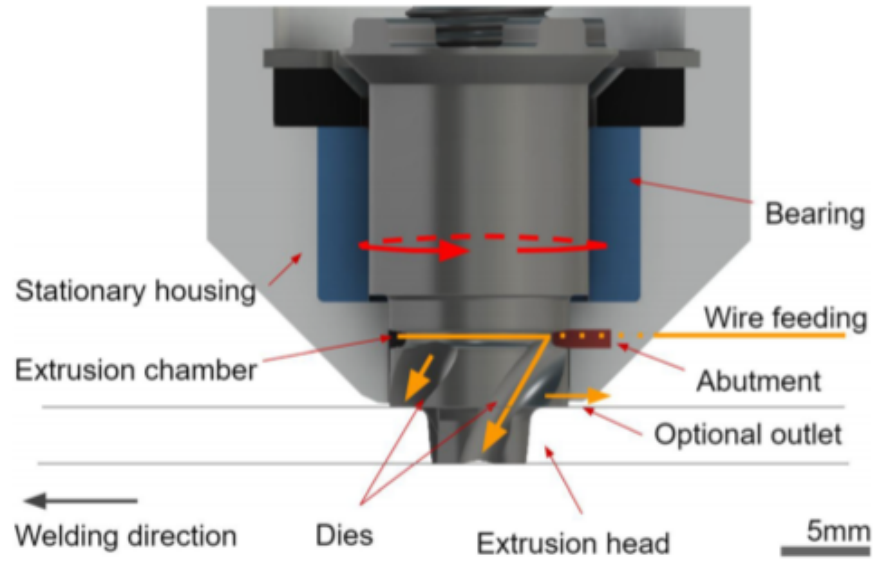


Figure 3: HYB machine illustration[14]

Friction is generating heat and plasticising the BMs. Almost all the mechanical work applied on the metals is converted to heat, approximately 95%. The CO₂ cooling system shown in Figure 4 allows most of this heat to be absorbed by the extrusion head[14] which has a positive effect, reducing the HAZ. When the FM is being extruded through the extrusion head, it plasticises together with the BMs. This in turn makes it possible for the filler to bond with the BMs[15]. Furthermore, the FM takes a lot of the deformation in the weld process which would otherwise be applied to the BMs. This makes the weld process more flexible and less susceptible to undercuts and other weld defects when compared to more conventional solid state joining techniques. An important factor when the weld is of dissimilar metals, is where the BMs are placed with regard to the pin rotation and welding direction. The side which makes contact with the pin having the same rotation direction as the welding direction, is called the advancing side. The side which makes contact with the pin having a rotation direction opposite of the welding direction is called the retreating side. Except for cold roll welding, reports on operating temperature, measures lower for HYB than other solid joining processes, which includes the often compared friction stir welding method[16].

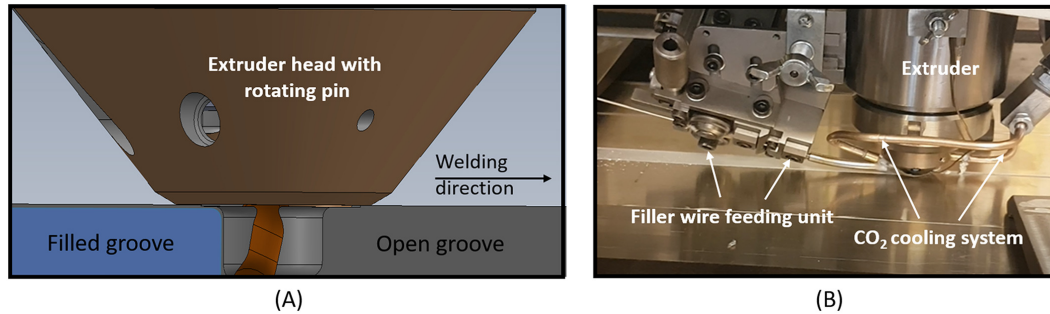


Figure 4: HYB machine illustration (A) and picture (B)[14]

2.1 HYB accomplishments

A butt weld between two cold rolled aluminum alloy 6082-T6 using the HYB method has been analyzed and compared to the gas metal arch weld and FSW methods. The two plates were 4 mm thick using a 1.2 mm diameter wire as the FM. The FM was of the type AA 6082-T4. Full metallic bonding was reported by the use of tensile testing reporting a fracture 4 mm offset from the weld center, Charpy V-notch testing and a scanning electron microscope (SEM) investigation. Charpy V-notch testing also reported the weld having a positive effect on the impact toughness. The HAZ softening weakened the BMs drastically with a reduction in yield strength of 47 %. The compared Gas metal arch weld and FSW had a reduction of 34 % and 43 % respectively. The study concluded the HYB outperformed the comparable gas metal arch weld and had a worse performance than the FSW, showing a good performance in similar metal Al bonding[17].

HYB found success when welding dissimilar materials. Aluminum alloy 6082-T6 to structural steel 355 have been successfully joined together using HYB for the first time in 2018[18]. Berto et al. created a joint where IMCs and oxides could not be seen when analyzed by SEM. The lower limit of SEM is $0.1\ \mu\text{m}$, hence the IMC thickness is less than $0.1\ \mu\text{m}$. Interestingly, the steel is unaffected by the process in terms of mechanical properties adding nothing to the HAZ width meaning all HAZ is in the EZ and Al BM part of the joint. HAZ width in the HYB weld is around 14mm. The low IMC thickness managed to partially hold during tensile testing breaking in the top part of the weld. Most of the fracture was reported to occur in the Al FM, but very close to the interface. Tensile strength measured at 140 MPa which is 45 % of the Al BM[18].

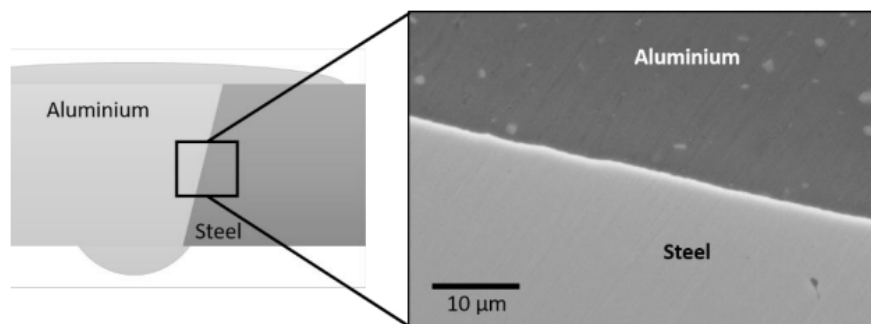


Figure 5: Interface between the first generation Al to steel weld[18]

A second generation Aluminum alloy 6082 to structural steel 355 HYB weld was made and studied. The results show a positive evolution in the the mechanical properties from the previous Al-steel joint study. This time the weld was analyzed with Transmission electron microscope (TEM) and SEM. Hardness tests measured a HAZ at around 15.5 mm with the steel being unaffected. TEM showed an IMC phase on the interface, but it was not continuous. The thickness varied from 0 to 50 nm with the presence of microscale mechanical interlocking. Like the first Al to steel

HYB weld, fracture occurred close to the Al-steel interface when tensile testing. Strain was observed in the Al HAZ during tensile testing, but due to cracks in the root area, fracture occurred on or close to the interface. However, the strength at tensile testing had increased from the previous 140 MPa to 184 - 220 MPa, equivalent to 60 - 72 % of the Al BM.

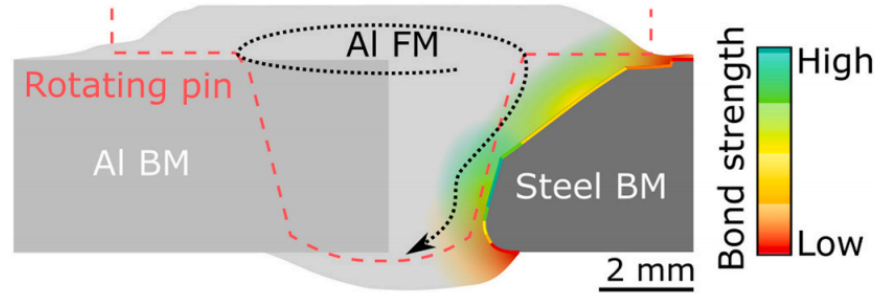


Figure 6: Strength in the interface of the Al to steel second generation HYB weld[19]

An aluminum alloy 6082-T4 to titanium grade 2 (Ti) weld was produced in a master thesis by Hursanay Turgun. Analysis in the form of SEM on the microscale, TEM on the nano scale and mechanical properties were conducted on the specimen. The thesis concluded there was no significant pores looking at the SEM analysis. The SEM also showed that fragments of titanium had dispersed into the Al. Vickers hardness measurements showed strain hardening for the BM Ti close to the interface caused by the HYB process. TEM showed the Ti and Al mixed in large areas on the interface. The formations indicates mechanical interlocking with a Al-Si-Ti IMC layer. The IMC layer measured at 51 ± 4 nm. Comparing the thickness to other Al-Ti welding techniques, the HYB method performs very well. Ultimate tensile tests showed a 305 ± 1 MPa with the fracture comfortably within the Al BM, therefore concluding an excellent bond for the interface [20]. The same thesis analyzed an Al - Cu HYB weld, but unfortunately due to the nature of the joint, Cu had to be on the receiving side. This created larger weld defects rendering the bonding faulty. However analysis on IMC was conducted observing the IMC thickness through high-angle annular dark field scanning-TEM. Thickness measured on three different sites on the weld, and showed a thickness of 260 ± 43 , 217 ± 51 and 200 ± 44 nm respectively[20].

3 Other weld methods

3.1 Diffusion welding

Diffusion bonding is a cold state welding technique using temperature and pressure to create a bond. Two surfaces are pressed together in conjunction with a temperature of $0.5 - 0.8 T_m$ (absolute melting temperature)[21]. The process enables similar and dissimilar metals to join, and the procedure varies depending on the materials used. The different parameters include applied pressure, time and bonding temperature[22]. Diffusion welding has performed well with avoiding cracks, distortion and segregation in dissimilar metal welds[23]. A schematic overview is illustrated in Figure 7.

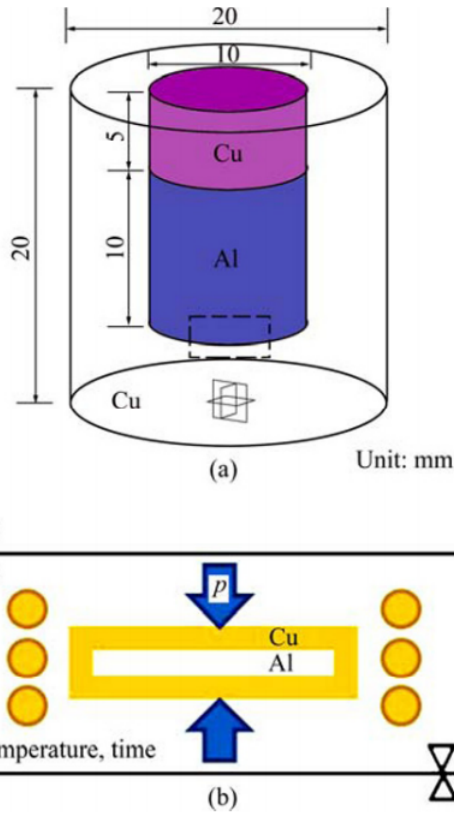


Figure 7: Diffusion welding schematic drawing. Al/Cu couple (a) and vacuum hot pressing (b)[24]

The variety of uses for diffusion welding has made it a candidate for Al - Cu welds. The problem however is the IMCs. The process requires high temperature over time which will increase the growth of IMCs leaving the tensile strength of the joint the same as the IMC interface, which is far below the Al BM[25]. Lee et al. studied an Al - Cu diffusion welding in vacuum, and found the best bonding temperature to be 545°C with a pressure time of 10 minutes and deformation rate of 0.2 mm/min. The SEM analysis showed bonding creating a three layered IMC interface reaching a total thickness of $15.06 \pm 0.94 \mu m$, way above the critical limit of $2 \mu m$. The report concluded the method to be feasible although more work is needed for the technique[24].

3.2 Ultrasonic welding

Ultrasonic welding is a welding technique utilizing vibration and pressure to bond materials. The vibrations are ultrasonic, meaning the frequency are above the ear's audibility limit (20 kHz or above). The pressure is used to bond and hold the pieces together. It is a solid state method which converts the vibration into energy that is applied on to the work pieces. Ultrasonic welding is used to bond similar or dissimilar metals. The technique has proved to work on various materials such as aluminum, copper, brass, silver and gold[26]. A schematic overview is illustrated in Figure 8.

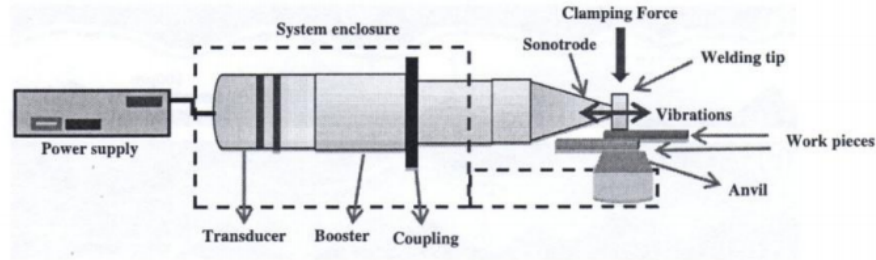


Figure 8: Ultrasonic welding schematic drawing[26]

Al - Cu ultrasonic welding poses its own challenges. Without using an interlayer, Al and Cu will not be able to have a continuous bond line. The Al will deform at a larger rate creating gaps along the interface. The Al will deform more using an interlayer as well, but the interlayer will be able to fill the gaps and continuous bonding has been reported. This is demonstrated in Figure 9. Ni and Ye bonded Al - Cu using ultrasonic welding. In their case, increasing the clamping pressure up to 60 psi allowed the bond to become mechanically stronger. Afterwards increasing pressure deteriorated the bond strength. Peak lap shear tensile strength was reported to be 73.4 MPa at 60 psi. A strain softening is observed in the weld area, however, 60 psi had a greater strain softening compared to the 40 psi weld. Ultrasonic welding is widely used in electronics, but it's currently not capable of handling as large joints as other solid weld techniques[27].

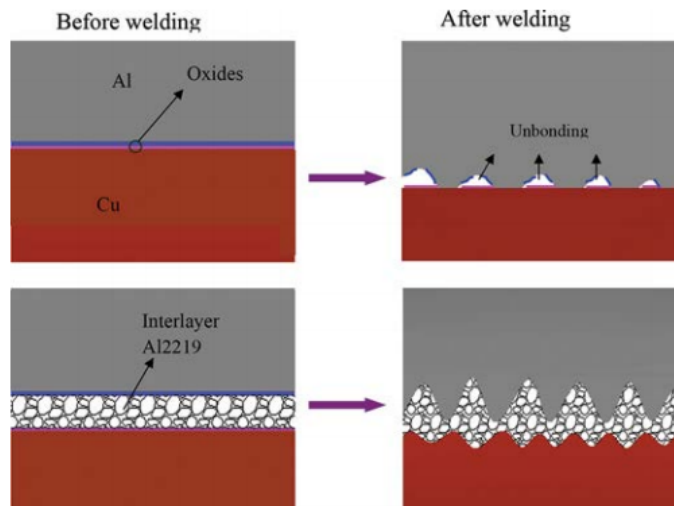


Figure 9: Ultrasonic welding schematic illustration of the bond line[27]

3.3 Friction stir welding

Friction stir welding (FSW) is a relatively new welding technique being invented in 1991 at the welding institute. The technique has served a purpose in similar metal Al fatigue and fracture resistant welds for aerospace. Al that are highly alloyed has been considered non-weldable in conventional weld methods due to the poor solidification, microstructure and porosity in the fusion zone. This creates a big loss in the mechanical properties when compared to the base metal. FSW was able to solve this problem and create solid welds between highly alloyed Al. A rotating tool is used which consists of a pin and a shoulder. Two abutting plates or sheets are held into place while the rotating tool is pressed down in to the abutting edges. The pin and shoulder is designed specifically to create suitable material flow and downward pressure. The purpose of the tool is in two parts, creating heat due to the friction and creating material flow due to the pin geometry[28].

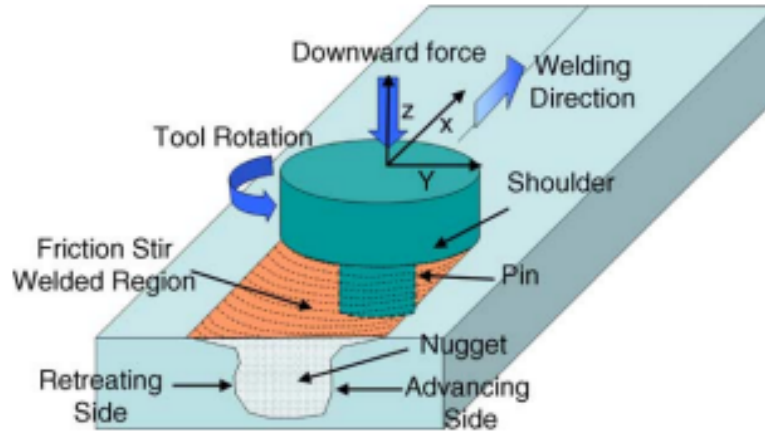


Figure 10: FSW schematic drawing[28]

FSW has shown promising welds in both Al to steel[29, 30] and Al to magnesium[31]. FSW is now being widely studied to be a suitable weld method for Al and Cu[32]. During FSW process, the material is experiencing large plastic deformation. Cu is the harder material and isn't deforming as much as the Al. This creates a situation where the Al has to cover more of the stir zone than Cu, creating a problem similar metal FSWs does not have. Saeid et al. conducted Al - Cu FSWs at a constant rotating speed of 1180rpm. His experiments shows the creation of cavities at higher weld speeds and microcracks at lower weld speeds, in the weld interface[32].

Ouyang et al. carried out experiments with Al - Cu FSW at different weld speeds and rotating speeds. They reported a large amount of material flow which in turn created a large amount of thick IMC layers. The main IMC compounds found were, $CuAl_2$, $CuAl$ and Cu_9Al_4 . This made the welds too brittle and considered unsound[33]. HAZ is determined from hardness tests showing a strain hardening on the Cu and strain weakening on the Al. HAZ shows a strain weakening in Al reaching 11 mm from the weld center. The stir zone always show a spike in hardness due to the creation of brittle and hard IMCs. The hardness in the stir zone are higher than both the Al and Cu BMs. The hardness measured in the stir zone varies considerably depending on the weld parameters such as the pins rotational speed[3]. Further work is required for the method and a suggestion is to introduce some kind of interlayer to produce a sound weld[33].

3.3.1 Flow Patterns in FSW

On bi metals, the materials will flow into each other. In the case of Al and Cu, the Cu will penetrate into Al in vortice shapes. There is also vertical flow since the material is usually pushed down by the threads in the tool[34], as a left handed thread pin rotating clockwise would. If the rotation would change, the material would be pushed up and the weld quality generally suffers. Material in the upper third part of the weld moves due to the influence of the shoulder and not the pin. The bottom two thirds of the weld is deformed by the pin itself. The material on the advancing side become very deformed and sheds off curving behind the pin ending up in curve shapes, often ending up going around the pin and ending up on the retreating side. Material on the retreating front side of the pin does not rotate around the pin, but is entrained and ends up on the retreating side in the pins wake while some reaches the advancing side[34]. The Cu should be placed on the advancing side even though it gets heavily deformed. This is because it is preferable that the hard Cu particles deposits on the retreating side. Cu particles depositing on the advancing side will create voids commonly called tunneling defect in FSW.

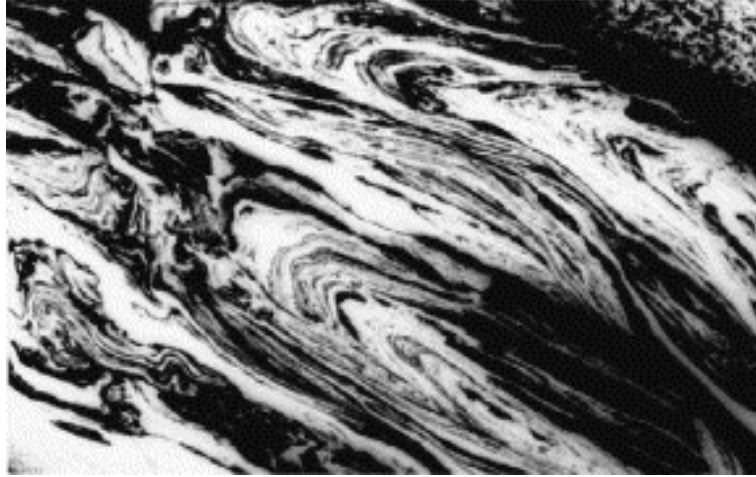


Figure 11: Al - Cu FSW material flow at the μm scale, vortices being roughly $40\ \mu\text{m}$ across. Light regions is Cu and Al is dark[34]

3.4 Cold roll welding

Cold rolling uses pressure followed by an annealment process to bond bimetallic joints in the form of plates or sheets. A roll with a fine surface rolls over the joint deforming the metals. The process has a threshold reduction between 40 % and 80 % at an applied pressure of 1000-3400 MPa. Illustrated in Figure 12, the material first has to go through a preparation to remove surface contamination. The surface contamination consist of oxides, humidity, grease, dust particles and absorbed ions. Second, the materials has to be aligned, stacked and fixed. Thirdly, the roll presses down onto the aligned and stacked metals while it rolls over.

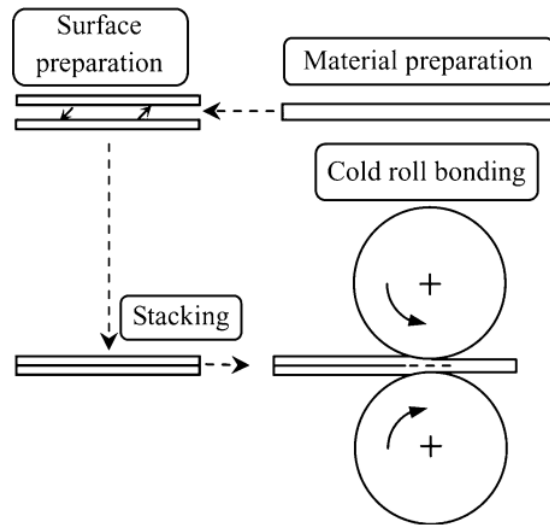


Figure 12: Cold roll weld schematic drawing[35]

Because of the nature of the joint, peeling force is the standard for measuring the mechanical strength. Peeling force defines how much combined adhesive, tensile strength and shear resistance the joint inhibits. Peeling force is derived from equation 7.

$$F_b = \frac{\bar{F}}{L_b} \quad (7)$$

F_b = Peeling force (N/cm)

\bar{F} = Mean tearing force (N)

L_b = Length of the bond (cm)

Chen et al. shows a strong correlation between peeling force and threshold reduction in Al - Cu cold roll welds, reporting a 32.3 N/cm peeling force at a 45 % reduction, 65.9 N/cm at 57 % and 107 N/cm at 66 % [36]. Abbasi et al. managed a peeling force of 180 N/cm at a 72 % threshold reduction with an Al - Cu cold roll welded joint [4]. Pre annealing, cold roll joints shows no presence of interdiffusion between the metals and different annealing parameters has been analyzed to create a sound bond. Due to the acceleration of interdiffusion rate caused by temperature, a critical IMC thickness can be reached in seconds or days depending on the annealing temperature [4, 36, 37]. If the IMC width reaches a thickness of 2.5 μm for this process, the bond has become brittle illustrated in Figure 13.

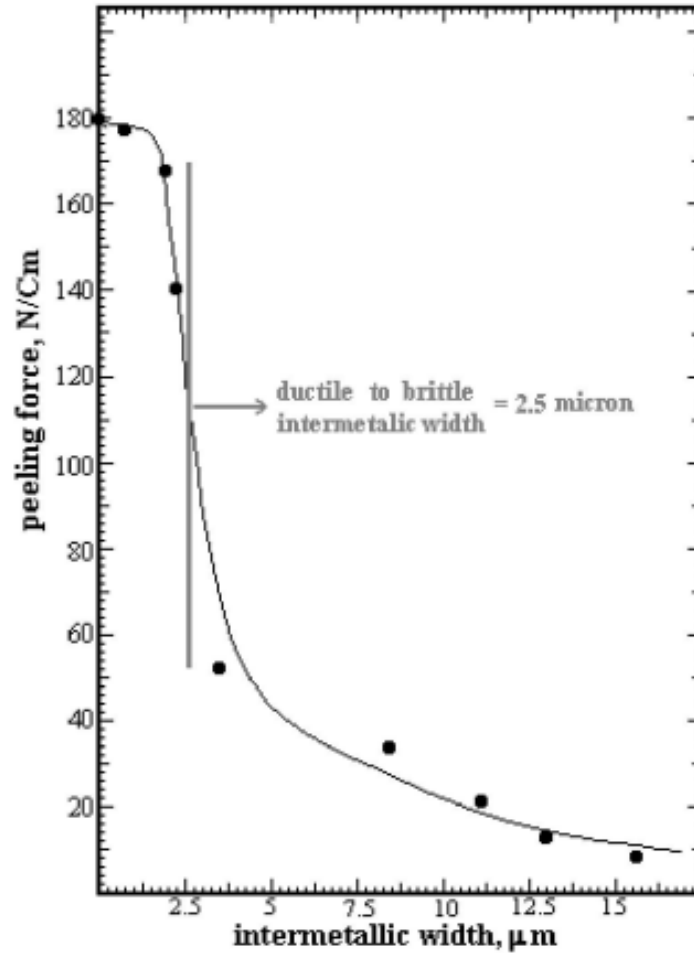


Figure 13: Cold roll weld, peeling force to IMC width graph [4]

Sheng et al. reached a sound bond annealing the rolled stack at a temperature of 145 $^{\circ}\text{C}$ for 20 hours [37]. TEM analysis confirmed the IMC thickness to be on a nanoscale. Cold roll welding is widely used in Al - Cu welding and it has proven to create sound bonding with IMC width below the 2 μm critical limit and a high peeling force [4, 38, 36, 37].

An advantage to the cold roll welding is the possibility to decide how large the contact area is for the joint. A larger contact area to a certain degree, reduces the resistance in the joints interface. There are however some drawbacks due to the great deformation in cold roll welding which can create stacking faults, dislocation and crystal defects, for instance twinned crystals[37]. Although most defects are detrimental to conductivity, high density twinned crystal in Cu is reported to have a high strength and conductivity which can be a neutral factor or even benefit the soundness of the bond[39].

4 Experiments

Experiments were carried out. One weld from the HYB process was tested on hardness along the the cross section of the weld. The goal of the experiment is to measure the hardness from the base metal on one side, through the weld and on to the other base metal, covering the width of the HAZ. The hardness test gives data on how the material property is, and how it changes compared throughout the weld. From that, we can determine the characteristics of the HAZ and it will give us an indication of the tensile strength, and where it is weakest and strongest. A digital microscope was used to observe the material flow in the EZ and possible large defects. Preliminary tests on conductivity was also conducted which is added to this report.

4.1 Vickers hardness

Hardness is defined as the ability to resist plastic deformation and the Vickers hardness test is one way to measure the hardness of the material. The hardness is measured by indenting a pyramid shaped diamond onto the specimen. This creates a square indentation that is measured by the length of both diagonals to get the area of the indent. The indenter is pressed down by a constant force and held for a set amount of time[40]. This report used 4 seconds to press down a 1 kg force. The force was subsequently held for 8 seconds before the release lasting another 4 seconds. According to the standard, 1 kg force gives a 1 HV deviation. The unit of hardness this method produces is Vickers Pyramid Number (HV) and Diamond Pyramid Number. Vickers hardness is calculated by equation 8,9.

$$HV = \frac{\text{Test force}}{\text{Surface area}} = \frac{F_{(kgf)}}{A_{S(mm^2)}} \quad (8)$$

$$A_S = \frac{d_v^2}{2\sin\frac{\alpha}{2}} \quad (9)$$

d_v = the mean of the two diagonals

α = the face angle of the diamond indenter

4.2 Digital microscope and hardness testing

4.2.1 specification

One aluminum alloy 6101 - Cu HYB weld with a plate thickness of 3 mm and a width of 25 mm was tested. The weld parameters were the following, a pin rotation of 350 RPM, weld speed set to 12 mm/s and a 4 mm gap between the Al and Cu BMs. The Mitutoyo MicroWiZhard hardness testing machine was used in conjunction with the standard ASTM-E92-17[41].

Alloy	Si	Fe	Cu	Mn	Mg	Cr	Zn	Ti	B	Others
6101	0.3-0.7	0.5	0.1	0.03	0.35-0.8	0.03	0.1	-	0.06	0.1

Table 3: Chemical composition shown in weight percentage with maximum amount, or minimum to maximum

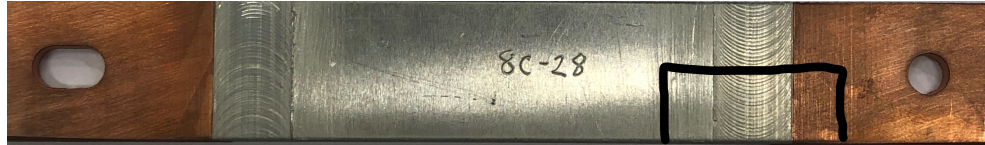
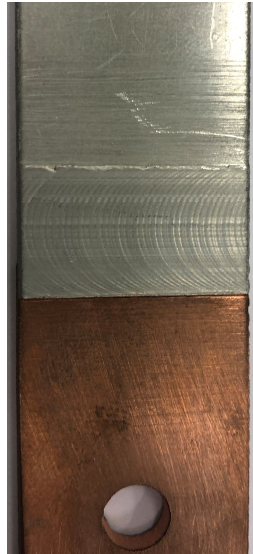


Figure 14: Front side of weld AA6101 with an outline in black of the test piece cut out



(a) Front side of the weld



(b) Back side of the weld

Figure 15: AA6101 test piece close up

4.2.2 Procedure

The test piece was ground down and then polished before both hardness testing and observing in the microscope. A test piece was cut from the weld and molded in epoxy resin to ensure an even grinding job as well as helping with stabilizing the test piece during testing. The piece was ground down gradually from a paper finish of 80, 220, 500, 1000, 2000, 4000 to $3\ \mu\text{m}$. Between each paper, the piece was rinsed off with water and alcohol, then blow dried. Constant monitoring of the grinding job was done to ensure an even grinding job. The finer paper seemed to be transporting small fragments of Cu on to the Al side so special precautions had to be made in regard with how to hold the specimen. This made it a bit more difficult to grind evenly. With the technique of always placing the Cu on the far side of the grinding/polishing plate, the amount of Cu on the Al side was reduced. Most of the Cu contamination was removed during polishing.

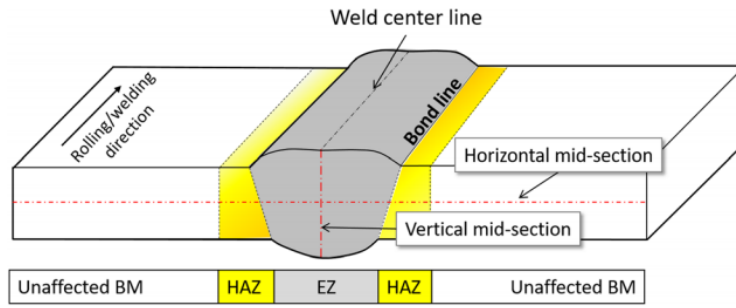


Figure 16: HAZ illustrated with center line and cross section[16]

After polishing, the specimen was ready for hardness testing and the digital microscope. The center of the weld was identified and indentations were carried out starting with one indent where the horizontal mid-section crosses the vertical mid-section lines. Thereafter twenty indents towards each side along the horizontal mid-section was made resulting in a total of forty one indents. The space between each indent was 0.5 mm. After indentation, the specimen was ground down enough for the indents to be gone, thereafter grinding and polishing steps were repeated to conduct another test. Three tests were conducted to ensure reliable results. These were plotted into a single graph shown in Figure 20.



Figure 17: Indented test piece in resin

4.2.3 Results

Optical microscopy The lighter Al in Figure 18,19 is the BM while the darker is the FM. The dark spots in the EZ are cavities. Cu has been on the advancing side which is crucial. The metal on the retreating gets more deformed and is more prone to pores. Al is the softer more suitable metal for the retreating side. Welds where Cu is on the retreating side creates microscopic pores and a very poor bond[20].



Figure 18: HYB weld showcasing material flow



Figure 19: Close-up

Difficulties during grinding dispersing Cu into the EZ and as far as the Al BM, created problems with regard to identifying if Cu has dispersed during welding. The digital microscope showed small amounts of Cu dispersed into the Al, but it is believed to be a grinding/polishing error. The weld is strongest when the IMC zone is located only on the Al - Cu interface. The dispersed Cu in FSW has shown to be a problem of creating brittle IMC zones inside the Al base metal. TEM and SEM analysis is required to conclude whether the IMC zone is localized to the interface or if Cu has dispersed into the EZ during welding.

Material flow is shown where the filler is pushed downwards in vortices being the thinnest in the middle and thickening towards the bottom. Excess filler is driven upwards protruding on the top. Al is clearly deformed together with the FM and Cu seems to be unaffected geometrically. Cavities are observed in the EZ. It is uncertain whether all are weld defects or if some are due to dispersed Cu creating some during grinding. However, some of the cavities did not disappear during grinding indicating that some are from the welding process.

Hardness test The hardness tests managed to determine the hardness of both base metals as well as determining the weld's HAZ. A graph is made with the three tests color organized with blue, orange and green. It shows a variance in the hardness results, but towards the base metals the variance seems to diminish.

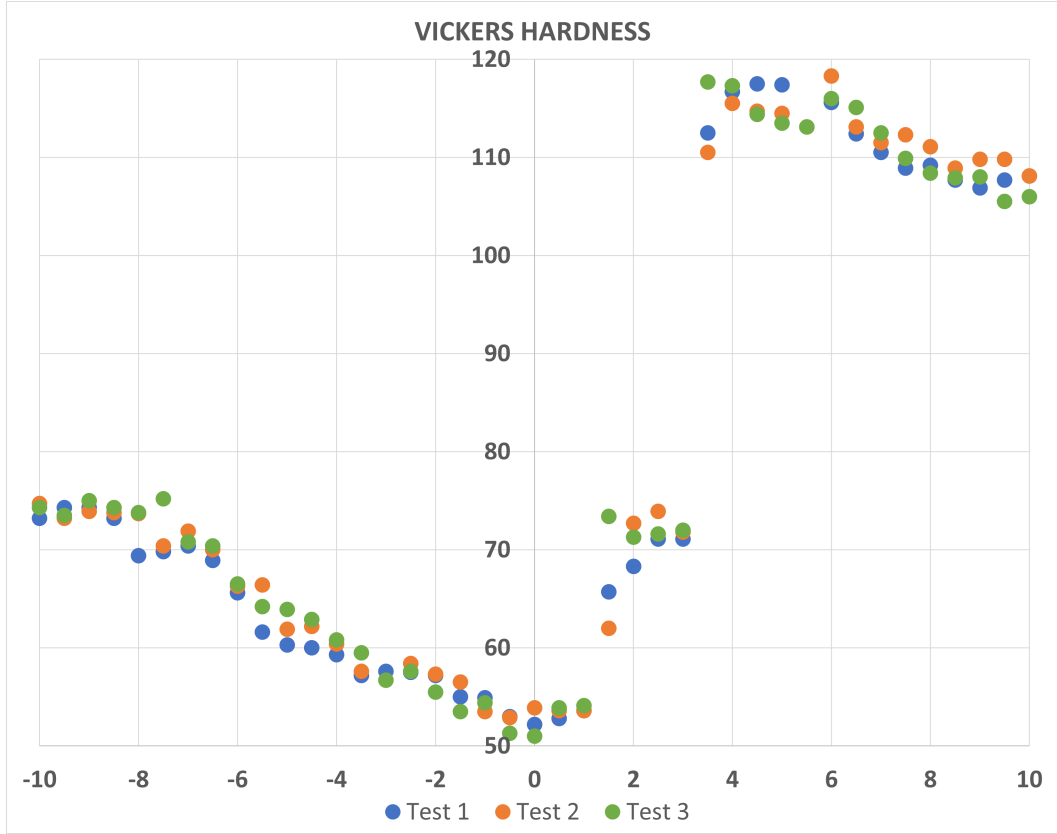


Figure 20: Results from three Vickers hardness tests with mm in the x-axis and HV in the y-axis, plotted

To make a more comprehensible a graph. A graph with the mean results with standard error bars was made. The standard error for the plot on each point of the weld was calculated using equation 10, 11.

$$S = \sqrt{\frac{\sum (X_i - \bar{X})^2}{N}} \quad (10)$$

S = Standard deviation

X_i = Specific value from population

\bar{X} = Mean value from population

N = Total population, which is equal to three on all cases

$$SE = \frac{S}{\sqrt{N}} \quad (11)$$

SE = Standard error

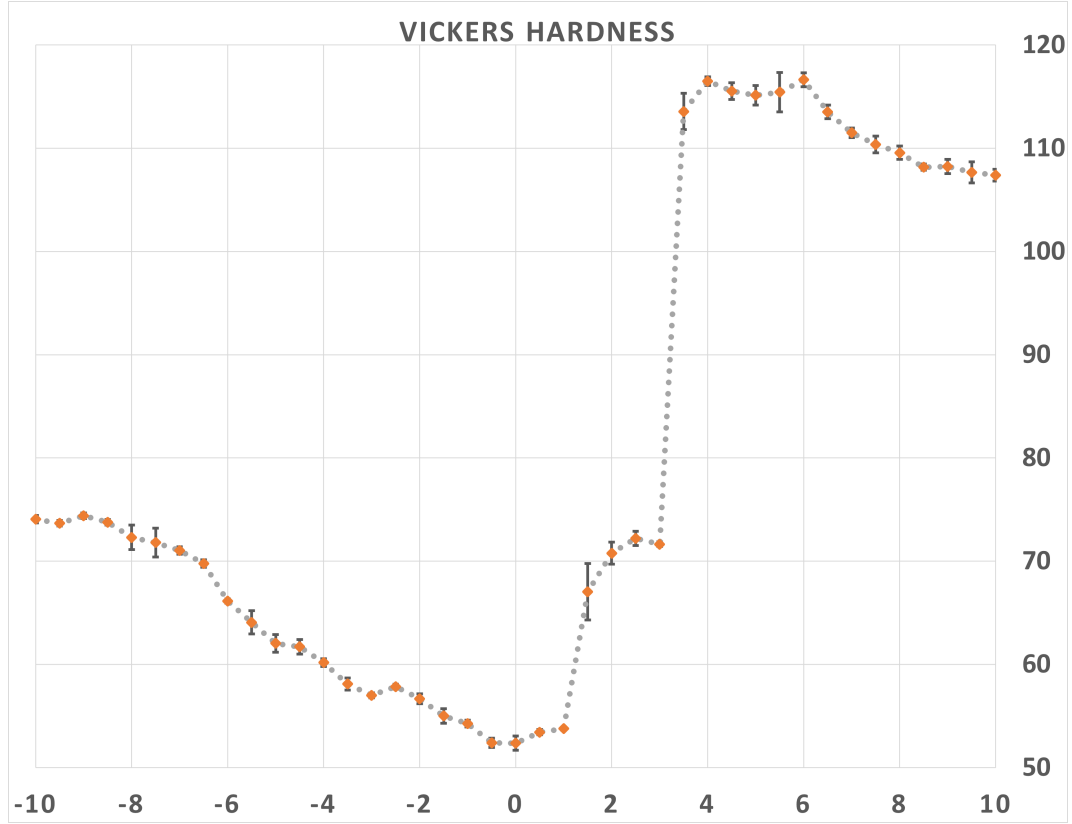


Figure 21: Results from three Vickers hardness tests with mm in the x-axis and HV in the y-axis with standard error bars

As shown in Figure 21, the 3.5mm plot is the last indent which is placed on the Al/EZ. This was also observed in the microscopy when doing the test and indicate a successful placement of the starting test position on all three tests. An amount of strain hardening on the Cu is observed in the HAZ while the Al is experiencing a strain softening. Five hardness values measured for each BM concluded a 74.04 HV for BM Al and 107.9 HV for BM Cu. HAZ reaches 8.5 mm into the Al BM from the weld center and 9.5 mm into the Cu side from the weld center. This results in a total HAZ of 18 mm, however, the strain hardening is affecting the tensile strength positively which could be benefiting the joint. HAZ reaches 6 mm into the Cu from the weld interface. The weakened HAZ is therefore 12 mm. Furthermore, the lowest hardness value is on the weld center. Hence, given a sound interfacial bond, fracture should occur in the weld center when tensile testing the joint. Also, none of the indents hit any cavity or defect observable in the microscope when testing.

4.3 Conductivity

It is interesting to add results for a preliminary conductivity test. A test was conducted on the HYB weld measuring the resistance over the weld. Resistance was measured from 5 mm on the Al side to 5 mm on the Cu side making a total bulk length of 10 mm. Resistance measured was $R = 3.401 \mu\Omega$ through the bulk. At a plate thickness of 3 mm and width of 25 mm, cross section area was calculated to be 75 mm^2 . Using equation 3 resistivity (ρ_{HYB}) is calculated.

$$\rho_{HYB} = 3.401 \cdot 10^{-6} \Omega \cdot \frac{0.01m}{75 \text{ mm}^2} = 0.02551$$

Inverse of the resistivity gave a conductivity of $39.204 \text{ m}/\Omega \text{ mm}^2$. These results give an indication of the electrical performance the joint inhibits, which are very promising when compared to IMC resistivity theory.

5 Conclusion

Creating a metallurgical bond between Al and Cu has proven difficult due to the brittle properties of the IMC phases. Bond strength are rapidly deteriorating after an IMC thickness of $2\text{ }\mu\text{m}$. The reported welding techniques have shown promise with regard to Al - Cu bonding, including HYB. All techniques have been able to create a bond, but the quality varies. Cold roll welding is used in practice with good results in the literature. The method can control the amount of interdiffusion and scores better than both FSW and diffusion welding with regard to IMC thickness. HYB in turn measured an IMC thickness on the nanoscale with unfavourable weld conditions having Cu on the retreating side. Preliminary conductivity tests also indicates a small IMC layer in the tested joint. Nevertheless, TEM analysis is required to determine how thick and consistent the IMC bond is.

For HYB, the digital microscope was not able to show a dispersing of Cu into the Al side, hence an analysis on the μm scale using SEM is needed to observe any dispersing of Cu fragments. Strain hardening for Cu and strain softening for Al was observed on the Al - Cu HYB weld. A relatively even spread of hardness values is seen on the BMs, but the EZ has a higher variance most likely due to the flow of FM and Al BM. HAZ is determined to be 18 mm whereas 6 mm of those resulted in a strain hardening. No spike in the weld center concludes HYB does not suffer the same problem as the FSW brittle and hard stir zone. HYB has created a bond and demonstrates great potential for the future of this technique in Al - Cu welding. It is versatile with regard to joint geometry being able to produce butt, corner and tee joints with modifications to the system. Nevertheless, cavity defects were detected and further analysis and understanding is needed to characterize the joint better.

5.1 Further work

1. Practical issues like the grinding and polishing, made an even grinding job and the observation of defects more difficult. Cu dispersing when grinding and small holes created during extended amounts of polishing were both issues that ideally should have been resolved. Improving this part will ease the observational tests.
2. Conductivity tests are of great interest. Mentioned previously, other weld methods conductivity are known as well as the theoretical best possible conductivity for an Al - Cu joint. HYB will be able to measure itself against other weld methods. This report's conductivity test is not conclusive and further testing is required.
3. Tensile testing are of great relevance. Bus bars might be under stressful conditions making a sound mechanical bond necessary. Tensile testing bimetallic welds are possible and preferable with the assist of camera vision. Mechanical properties are also strongly tied to the conductivity performance which will add more confidence to the conductivity tests.
4. A bus bar might be located on a ship with high amounts of vibrations and harsh corrosion environments. The method will benefit from characterizing what weaknesses it has with regard to these factors. Fracture mechanic evaluation and corrosion testing is therefore preferable when deducing the practicality of the technique.
5. TEM and SEM analysis will allow a greater understanding of the Al - Cu bonding. It will be able to identify the IMC characteristics with regard to thickness, phases and placement. Other properties of the weld such as dispersing of Cu, kissing defects or mechanical interlocking will be identifiable as well.
6. Iterating the weld parameters to create a more sound weld. Al - Cu bonding with the HYB method is relatively new. This report being the first one to showcase the material flow and hardness measurements of an Al - Cu weld where the Cu is on the advancing side. That being said, the digital microscope is showing weld defects that indicates that some iteration to the weld parameters might be warranted.

References

- [1] Jean Pierre Bergmann, Franziska Petzoldt, Renè Schürer, and Stefan Schneider. Solid-state welding of aluminum to copper—case studies. *Welding in the World*, 57(4):541–550, 2013.
- [2] William E Veerkamp. Copper-to-aluminum transitions in high dc bus systems. *IEEE transactions on industry applications*, 33(4):1027–1034, 1997.
- [3] Nidhi Sharma, Arshad Noor SIDDIQUEE, et al. Friction stir welding of aluminum to copper—an overview. *Transactions of Nonferrous Metals Society of China*, 27(10):2113–2136, 2017.
- [4] M Abbasi, A Karimi Taheri, and MT Salehi. Growth rate of intermetallic compounds in al/cu bimetal produced by cold roll welding process. *Journal of Alloys and Compounds*, 319(1-2):233–241, 2001.
- [5] Saleem Hashmi. *Comprehensive materials processing*. Newnes, 2014.
- [6] Milenko Braunovic and N Aleksandrov. Effect of electrical current on the morphology and kinetics of formation of intermetallic phases in bimetallic aluminum-copper joints. In *Proceedings of IEEE Holm Conference on Electrical Contacts*, pages 261–268. IEEE, 1993.
- [7] Won-Bae Lee, Kuek-Saeng Bang, and Seung-Boo Jung. Effects of intermetallic compound on the electrical and mechanical properties of friction welded cu/al bimetallic joints during annealing. *Journal of Alloys and Compounds*, 390(1-2):212–219, 2005.
- [8] Ji L Murray. The aluminium-copper system. *International metals reviews*, 30(1):211–234, 1985.
- [9] Norbert Ponweiser, Christian L Lengauer, and Klaus W Richter. Re-investigation of phase equilibria in the system al–cu and structural analysis of the high-temperature phase η 1-al1- δ cu. *Intermetallics*, 19(11):1737–1746, 2011.
- [10] Yu-chang Su, Jian Yan, Pu-tao Lu, and Ji-tao Su. Thermodynamic analysis and experimental research on li intercalation reactions of the intermetallic compound al₂cu. *Solid State Ionics*, 177(5-6):507–513, 2006.
- [11] EH Kisi and JD Browne. Ordering and structural vacancies in non-stoichiometric cu–al γ brasses. *Acta Crystallographica Section B: Structural Science*, 47(6):835–843, 1991.
- [12] LARS Arnberg and SVEN Westman. Crystal perfection in a noncentrosymmetric alloy. refinement and test of twinning of the γ -cu₉al₄ structure. *Acta Crystallographica Section A: Crystal Physics, Diffraction, Theoretical and General Crystallography*, 34(3):399–404, 1978.
- [13] FA Calvo, A Ureng, JM Gomez De Salazar, and F Molleda. Special features of the formation of the diffusion bonded joints between copper and aluminium. *Journal of materials science*, 23(6):2273–2280, 1988.
- [14] Øystein Grong, Lise Sandnes, and Filippo Berto. A status report on the hybrid metal extrusion & bonding (hyb) process and its applications. *Material Design & Processing Communications*, 1(2):e41, 2019.
- [15] Øyvind Frigaard, Øystein Grong, and OT Midling. A process model for friction stir welding of age hardening aluminum alloys. *Metallurgical and materials transactions A*, 32(5):1189–1200, 2001.
- [16] Lise Sandnes, Øystein Grong, Jan Torgersen, Torgeir Welo, and Filippo Berto. Exploring the hybrid metal extrusion and bonding process for butt welding of al–mg–si alloys. *The International Journal of Advanced Manufacturing Technology*, 98(5-8):1059–1065, 2018.
- [17] Lise Sandnes. Preliminary Benchmarking of the HYB (Hybrid Metal Extrusion Bonding) Process for Butt Welding of AA6082-T6 Plates Against FSW and GMAW . Master’s thesis, Norwegian University of Science and Technology, Trondheim, Norway, 2017.
- [18] Filippo Berto, Lise Sandnes, Filippo Abbatalini, Øystein Grong, and Paolo Ferro. Using the hybrid metal extrusion & bonding (hyb) process for dissimilar joining of aa6082-t6 and s355. *Procedia Structural Integrity*, 13:249–254, 2018.

- [19] Tina Bergh, Lise Sandnes, Duncan Neil Johnstone, Øystein Grong, Filippo Berto, Randi Holmestad, Paul Anthony Midgley, and Per Erik Vullum. Microstructural and mechanical characterisation of a second generation hybrid metal extrusion & bonding aluminium-steel butt joint. *Materials Characterization*, page 110761, 2020.
- [20] Hursanay Turgun. Electron Microscopy Characterization of Aluminium-Copper-Titanium-Steel Joint made using the Hybrid Metal Extrusion Bonding Method. Master's thesis, Norwegian University of Science and Technology, Trondheim, Norway, 2020.
- [21] B Ravisankar, J Krishnamoorthi, SS Ramakrishnan, and PC Angelo. Diffusion bonding of su 263. *Journal of materials processing technology*, 209(4):2135–2144, 2009.
- [22] Ho-Sung Lee, Jong-Hoon Yoon, Chan Hee Park, Young Gun Ko, Dong Hyuk Shin, and Chong Soo Lee. A study on diffusion bonding of superplastic ti–6al–4v eli grade. *Journal of Materials Processing Technology*, 187:526–529, 2007.
- [23] Y. Li and F. Lin. Customer segmentation analysis based on som clustering. volume 1, pages 15–19, 2008. cited By 3.
- [24] Kwang Seok Lee and KWON Yong-Nam. Solid-state bonding between al and cu by vacuum hot pressing. *Transactions of Nonferrous Metals Society of China*, 23(2):341–346, 2013.
- [25] Toshio Enjo, Kenji Ikeuchi, and Naofumi Akikawa. Diffusion welding of copper to aluminum (materials, metallurgy, weldability). *Transactions of JWRI*, 8(1):77–84, 1979.
- [26] Elma Kicukov and Ali Gursel. Ultrasonic welding of dissimilar materials: A review. *Periodicals of Engineering and Natural Sciences*, 3(1), 2015.
- [27] ZL Ni and FX Ye. Dissimilar joining of aluminum to copper using ultrasonic welding. *Materials and Manufacturing Processes*, 31(16):2091–2100, 2016.
- [28] Rajiv S Mishra and ZY Ma. Friction stir welding and processing. *Materials science and engineering: R: reports*, 50(1-2):1–78, 2005.
- [29] CM Chen and R Kovacevic. Joining of al 6061 alloy to aisi 1018 steel by combined effects of fusion and solid state welding. *International Journal of Machine Tools and Manufacture*, 44(11):1205–1214, 2004.
- [30] Won-Bae Lee, Martin Schmuecker, Ulises Alfaro Mercardo, Gerhard Biallas, and Seung-Boo Jung. Interfacial reaction in steel–aluminum joints made by friction stir welding. *Scripta Materialia*, 55(4):355–358, 2006.
- [31] Jiuchun Yan, Zhiwu Xu, Zhiyuan Li, Lei Li, and Shiqin Yang. Microstructure characteristics and performance of dissimilar welds between magnesium alloy and aluminum formed by friction stirring. *Scripta Materialia*, 53(5):585–589, 2005.
- [32] T Saeid, A Abdollah-Zadeh, and B Sazgari. Weldability and mechanical properties of dissimilar aluminum–copper lap joints made by friction stir welding. *Journal of Alloys and Compounds*, 490(1-2):652–655, 2010.
- [33] Jiahu Ouyang, Eswar Yarrapareddy, and Radovan Kovacevic. Microstructural evolution in the friction stir welded 6061 aluminum alloy (t6-temper condition) to copper. *Journal of Materials Processing Technology*, 172(1):110–122, 2006.
- [34] M Guerra, C Schmidt, John C McClure, LE Murr, and AC Nunes. Flow patterns during friction stir welding. *Materials characterization*, 49(2):95–101, 2002.
- [35] Roohollah Jamaati and Mohammad Reza Toroghinejad. The role of surface preparation parameters on cold roll bonding of aluminum strips. *Journal of Materials Engineering and Performance*, 20(2):191–197, 2011.
- [36] Chih-Yuan Chen, Hao-Long Chen, and Weng-Sing Hwang. Influence of interfacial structure development on the fracture mechanism and bond strength of aluminum/copper bimetal plate. *Materials transactions*, 47(4):1232–1239, 2006.

- [37] LY Sheng, F Yang, TF Xi, C Lai, and HQ Ye. Influence of heat treatment on interface of cu/al bimetal composite fabricated by cold rolling. *Composites Part B: Engineering*, 42(6):1468–1473, 2011.
- [38] Chih-Yuan Chen and Weng-Sing Hwang. Effect of annealing on the interfacial structure of aluminum-copper joints. *Materials transactions*, pages 0706110009–0706110009, 2007.
- [39] Lei Lu, Yongfeng Shen, Xianhua Chen, Lihua Qian, and Ke Lu. Ultrahigh strength and high electrical conductivity in copper. *Science*, 304(5669):422–426, 2004.
- [40] Mohammad Jawaid, Mohamed Thariq, and Naheed Saba. *Structural Health Monitoring of Biocomposites, Fibre-Reinforced Composites and Hybrid Composites*. Woodhead Publishing, 2018.
- [41] A Standard. Astm e92-17,“. *Standard test methods*.